

# **SIZING AND PERFORMANCE IMPLICATIONS OF A REGIONAL AIRCRAFT FOR INNER-CITY-AIRPORT OPERATIONS**

## **Philipp Heinemann**

Bauhaus Luftfahrt e.V.  
Willy-Messerschmitt-Str. 1, D-  
82024 Taufkirchen, Germany  
Philipp.Heinemann@bauhaus-luftfahrt.net

## **Michael Schmidt**

Munich Aerospace e.V.  
Willy-Messerschmitt-Str. 1, D-  
82024 Taufkirchen, Germany  
Michael.Schmidt@bauhaus-luftfahrt.net

## **Christoph Jeßberger**

Bauhaus Luftfahrt e.V.  
Willy-Messerschmitt-Str. 1, D-  
82024 Taufkirchen, Germany  
Christoph.Jeßberger@bauhaus-luftfahrt.net

## **Felix Will**

Technical University of  
Munich  
Boltzmannstraße 15, D-85747  
Garching, Germany  
Felix.Will@tum.de

## **Sascha Kaiser**

Bauhaus Luftfahrt e.V.  
Willy-Messerschmitt-Str. 1, D-  
82024 Taufkirchen, Germany  
Sascha.Kaiser@bauhaus-luftfahrt.net

## **Mirko Hornung**

Bauhaus Luftfahrt e.V.  
Willy-Messerschmitt-Str. 1, D-  
82024 Taufkirchen, Germany  
Mirko.Hornung@bauhaus-luftfahrt.net

**Abstract.** This technical work comprises an airport and aircraft symbiosis, designed to enable aircraft operation out of inner-city airports targeting the Advisory Council for Aviation Research and Innovation in Europe (ACARE) goals of a four hour door-to-door travel within Europe. The study is the result of an interdisciplinary group design project at Bauhaus Luftfahrt e.V. Shorter airport access and terminal processing times are seen as key enablers. During the development, a holistic view on the concept was ensured to allow the implementation in urban regions with the aim to relieve congested hub airports from direct passengers and aircraft movements and to permit faster travel times. The realization and operation within modern cities considers existing infrastructure. Space restrictions in city centers and the need for general acceptance from the public lead to demanding constraints for the overall aircraft design process. Combined with an economic market analysis, aircraft top level requirements were established that call for a low noise aircraft with Short Takeoff and Landing (STOL) capabilities.

The paper describes the methodical approach and iterative procedure of the design process. A detailed concept for a 60 passenger single aisle aircraft is proposed for an Entry-Into-Service year 2040 with a design range of 1,500 nautical miles for a load factor of 90 %. Although the design for STOL and low noise operation had to be traded partly with cruise efficiency, a noteworthy reduction in fuel burn per passenger and nautical mile could be achieved against current aircraft. An assessment of potential technologies is conducted to provide the required enhancements to fulfill of the abovementioned constraints. Operational procedures were analyzed to reduce the noise propagation through flight path optimization. Furthermore a ground based assisted takeoff system was conceived to lower required takeoff field length and to prevent engine sizing just for the takeoff case. Cabin design optimization for a fast turnaround has been conducted to ensure a wide utilization spectrum. The results prove the feasibility of an aircraft developed for inner city operation.

**Keywords.** Aircraft Design, Regional, STOL, Low Noise

# 1 Introduction

One major goal of the European Commission's Flight Path 2050 document is that 90% of travelers should be able to reach a destination within Europe in four hours from door to door [1]. This goal requires optimization with respect to both aircraft and airport technologies as well as a perfect fit of both. To this end, an interdisciplinary group design project at Bauhaus Luftfahrt was initiated to develop a feasible solution for the proposed goal. Within the project, a comprehensive study of a novel aircraft and airport concept has been conducted. Four key drivers are setting the scene of this group design project:

- (1) Four hours door-to-door travel time for inner-European flights and associated connecting transport modes needs to be achieved.
- (2) Different air traffic forecasts predict global growth rates to be around 4.7 % per year. Until 2040 this means that air traffic will triple. [2]
- (3) Urbanization and a growing number of megacities are already an important driver of today's transport challenges but will become even more important up to and beyond 2040 as raising agglomeration in cities is meant to result in a share of 2/3 of the global population to live in cities. [3]
- (4) The geographical location of airports as well as the related airport connectivity in combination with the ongoing agglomeration in megacities is a key challenge to meet the fast growing air transport demand until 2040 at these air transport nodes.

These key drivers indicate that there is a need for an air transport concept which is located near city centers, supports global air traffic growth and urbanization challenges and, thus, is a mass transportation mode connecting major city-pairs, and ensures door-to-door travel times of less than four hours.

For the 100 biggest cities in Europe, Asia and North America, available space was analyzed near the city centers which could be used as an inner city airport, called "CentAirStation". Spaces with sufficient dimensions had been found in each of the 30 biggest cities in Europe around six times on average (Table 2, overleaf). As most available spaces are located above train tracks of inner city train stations, such locations enable smooth connections from and to inner city transport modes. Therefore, a CentAirStation is a four level building with the train station on the 1<sup>st</sup> floor, a public level with shops and security checks on the 2<sup>nd</sup> floor, the apron level on the 3<sup>rd</sup> floor and the runway level on the roof. Passengers can board an aircraft via a gate on the apron level which is linked by security tunnels starting on the public level. Aircraft are moved by taxi robots from the gates on the apron level to one of the four elevators in each corner of the apron level up to the runway level. Further information regarding the CentAirStation concept can be found in [4]. In order to obtain public acceptance of aircraft movements in city centers, such aircraft need to reduce their negative impact, like CO<sub>2</sub>, NO<sub>x</sub> and noise emissions significantly. Thus, a novel and perfectly adopted aircraft – the "CityBird" – which can be operated at CentAirStations as well as at conventional airports was necessary.

The CityBird concept is described in detail in section 2 after the definition of aircraft top level requirements and a brief market assessment. Section 3 looks closely at the flight performance of a CityBird and section 4 concludes and gives an outlook to future work.

## 1.1 Aircraft Top Level Requirements

The definition of the aircraft top level requirements (ATLeRs) shows how many requirements and constraints were within the context of this project. In this section, the process of top level requirement definition is outlined. Since the aircraft aims to address mass transport for all passenger groups, the potential and the market size in terms of possible customers was analyzed. It also serves primarily as a city-to-city connection and aims to be a slot relief concept at major airports freeing up capacity for

further hub operations, especially on longer ranges. Therefore, economic considerations were taken into account. The growth of the aviation market was considered by using the average of eleven market forecasts [5] predicting growth until 2030 and an extrapolation towards 2040 on revenue passenger kilometers (RPK) for the economically most interesting regions in the world. This includes the North American continent, Europe and Asia. A worldwide growth rate of 4.7 % per year is expected. Table 1 shows the growth rate by region and the growth of frequencies and installed seats per aircraft taken as an average of the before mentioned aviation forecasts until 2030.

Table 1: Forecasted aviation growth [5]

| <i>Region</i>        | <i>Annual RPK Growth</i> | <i>Growth in Frequency by 2030</i> | <i>Growth in average installed seats by 2030 [6]</i> |
|----------------------|--------------------------|------------------------------------|--|
| <b>Europe</b>        | 4.1 %                    | + 40 %                             | + 7 %  |
| <b>Asia</b>          | 6.2 %                    | + 146 %                            | + 15 %   |
| <b>North America</b> | 3.0 %                    | + 36 %                             | + 5 %  |

An analysis from Official Airline Guide (OAG) of 2012 [7] data resulted in the number of offered RPK from every analyzed city pair with a range equal or lower than the desired design range of the aircraft concept. In combination with the forecasted growth rate, this led to design capacity of a CentAirStation of 10.5 million passengers per year. Assuming a 16 hour operation of the airport per day and a normal frequency for departures and arrivals at the airport, a capacity of 60 passengers per aircraft is deemed necessary. A more detailed analysis of the airport passenger capacity estimation can be found in [4].

To ensure interconnection of the most important cities within a region concerning passenger flow, the range had to be appropriately sized. An analysis shows the need for a 1,500 NM range to connect most of the major cities in the aforementioned three regions. Although the average stage length today flown by Airbus A320 in Europe is 480 NM for Low Cost Carriers, respectively 600 NM for Full Service Carriers [7], the high range for a regional sized aircraft is justified by the four hour door-to-door travel time, thus avoiding stop-overs which are time consuming. Although the A320 has a greater passenger capacity and range, it serves as a main city connector nowadays and is therefore suited for comparison.

The cruise speed is defined by the goal of a four hour door to door travel time and the range. This includes block time, boarding/deboarding times, time within the airport while arriving or departing, and time from the starting point of the journey to the airport and to the final destination. Hence, the airport and aircraft concept should be designed to shorten access times. Figure 1 shows the block time in relation to the flight distance for Mach numbers of M0.60 and M0.66 compared to a conventional profile flown by an Airbus A320 (M0.76). The diagrams show that an additional time of 48 minutes is needed for a 1,500 NM journey, if the cruise speed is M0.60 compared to an A320. For a cruise speed of M0.66 this is reduced to 28 minutes. The flight time for 1,500 NM exceeds the four hour goal already on block time. It is equal to four hours at 1,250 NM for M0.66 and 1,131 NM for M0.6. Not included are the times for the journey to and from the airport further lowering the 4-hour-range. Since the highest utilization is on stage lengths below 600 NM, the lower speeds compared to the A320 permit sufficient margin for most of the conducted flights. It was decided that a minimum cruise Mach number of M0.60 is necessary, while M0.66 would be the preferred cruise speed.

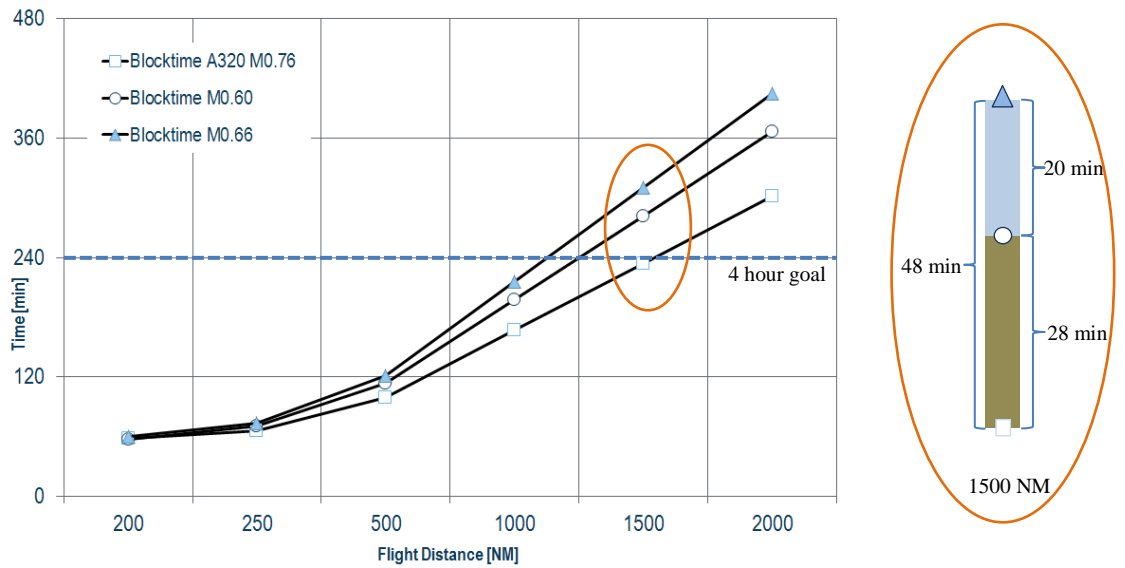


Figure 1: Change of block time for M0.60 and M0.66 compared to A320 mission (M0.76)

The analysis of available space within the major cities includes possible number of spaces and also their possible length and width of the runway (RWY) shown in Table 2. A deeper analysis was conducted to find the threshold at what length and width of a runway a potential city cannot provide the required space anymore. To minimize the number of these cities, the dimensions were chosen to be relatively low. The runway length was defined as 640 m and a width of 80 m. This width serves as the maximum width of the airport. The runway width amounts to 30 m. Furthermore the atmospheric conditions at which the aircraft has to comply with the requirement at Maximum Takeoff Weight (MTOW) was set at a pressure altitude of 2,000 ft and a temperature of ISA+10K to provide additional safety margin for operation on most airports.

Table 2: Overview of investigated data

| <i>Region</i>        | <i>No. investigated cities</i> | <i>Avg. number of potential airports</i> | <i>RWY length [m]</i> |             |            | <i>RWY width [m]</i> |             |            |
|----------------------|--------------------------------|--|-----------------------|-------------|------------|----------------------|-------------|------------|
|                      |                                |  | <i>Min</i>            | <i>Avg.</i> | <i>Max</i> | <i>Min</i>           | <i>Avg.</i> | <i>Max</i> |
| <b>Europe</b>        | 34                             | 5.8                                      | 570                   | 1341        | 5300       | 80                   | 124         | 500        |
| <b>Asia</b>          | 40                             | 3.6                                      | 600                   | 980         | 3000       | 80                   | 122         | 260        |
| <b>North America</b> | 25                             | 3.4                                      | 580                   | 1230        | 3000       | 80                   | 133         | 880        |

The definition of a requirement for the noise signature of the aircraft is based on the ICAO specifications and the Flightpath 2050 goals [1] that aim to reduce the perceived noise emission of flying aircraft by 65% compared to the year 2000. The limits active in the year 2000 are found in Chapter 3 of the ICAO Annex 16 [8] stating a cumulative noise level of 281 EPNdB for the MTOW-class of the aircraft. Since inner-city operations do most likely demand bigger noise reductions, it was decided to use the Chapter 4 values, active since 2006, as a baseline stating a limit of 255.6 EPNdB. Interpolating the goal defined by Flightpath 2050 for the year 2040 leads to a 52 % reduction which equals a cumulative noise requirement for the aircraft of 223.92 EPNdB consisting of 73.8 EPNdB for sideline, 69.4 EPNdB for flyover and 80.6 EPNdB for approach noise.

Summing up, the ATLeRs deemed necessary for the success of the aircraft are defined below.

- The vehicle must accommodate 60 passengers in a single class arrangement
- Maximum range not less 1,500 NM at a load factor of 90 % (54 PAX)
- Takeoff Field Length (TOFL) and Landing Field Length (LFL) less than or equal to 640 m (2,100 ft) at ISA+10K and a pressure altitude of 2,000 ft
- Cruise speed of not less than M0.6 on design range
- Time to climb to cruise altitude of no more than 25 minutes
- Cruise altitude higher than 31,000 ft to permit operational flexibility and overfly weather
- Maximum dimensions driven by airport apron space constraints [4] of 28 m wingspan and 24 m length
- Noise reduction by 52 % compared to the ICAO Chapter 4 (224 EPNdB)
- Certification rules according CS-25 and FAR 25 transport category
- Turnaround time of 15 minutes
- The vehicle must operate at conventional airports with no negative impact on processes and capacity and only minor infrastructural requirements
- Reduction of CO<sub>2</sub> by 55% compared to the year 2000 interpolated from the Flightpath 2050 [1] and SRIA [9] goals resulting from propulsion and airframe improvements

## 1.2 State of the Art Aircraft Assessment

During the definition of the ATLeRs, an analysis of existing aircraft with similar characteristics was performed to evaluate the design space of the concept. The aircraft analyzed are shown in Table 3.

Table 3: Statistical overview of regional aircraft in comparison with CityBird ATLeRs

| <i>Aircraft name</i>     | <i>PAX</i> | <i>Wing loading</i><br><i>[kg/m<sup>2</sup>]</i> | <i>TOFL</i><br><i>[m]</i> | <i>Cruise speed</i><br><i>[KTAS]</i> | <i>Range</i><br><i>[NM]</i> | <i>Cumulative noise</i><br><i>[EPNdB]</i> |
|--------------------------|------------|--|---------------------------|--------------------------------------|-----------------------------|---|
| <b>ATR 72</b>            | 68         | 360  | 1224                      | 275                                  | 785                         | 255                                       |
| <b>An 24</b>             | 50         | 280  | 1650                      | 257                                  | 1115                        | 274                                       |
| <b>Transall C-160</b>    | 77         | 318  | 751                       | 277                                  | 1000                        | -   |
| <b>Dash 8</b>            | 40         | 303  | 1300                      | 360                                  | 1362                        | 257                                       |
| <b>Fokker 50</b>         | 60         | 327  | 1050                      | 287                                  | 1110                        | 262                                       |
| <b>Dornier 328 Prop</b>  | 33         | 350  | 1088                      | 335                                  | 707                         | 261                                       |
| <b>Dornier 328 Jet</b>   | 33         | 392  | 1367                      | 398                                  | 950                         | 258                                       |
| <b>ATR 42</b>            | 48         | 306  | 1041                      | 270                                  | 456                         | 248                                       |
| <b>Mean</b>              | 51         | 330  | 1181                      | 307                                  | 936                         | 259                                       |
| <b>CityBird (ATLeRs)</b> | 60         | 350  | 640                       | 381                                  | 1500                        | 224                                       |

The table shows that the ATLeRs are comparable to other existing regional aircraft. The higher wing loading compared to the mean value combined with the low requirement for TOFL, which is almost half the average, as well as the noise limit poses the greatest challenges to this point. Furthermore the cruise speed is 74 KTAS above the average of the investigated aircraft. This is mainly due to the fact that most of the vehicles are turboprop aircraft and therefore operate in a slower cruise speed regime. To achieve these ambitious targets it requires the use of new technological advancements incorporated into the aircraft.

## 2 Concept Description

The aircraft concept features a tricycle, monoplane, twin-turbofan with podded mountings on the upper aft section of the fuselage and a U-shaped empennage. The low wing configuration is unswept with leading and trailing edge high lift devices along the whole span (excluding winglet). The pressurized fuselage requires a cockpit crew of two and the cabin accommodates two flight attendants. The aircraft has two type B exit pairs in the front and aft section and a small baggage compartment in the tail section of the fuselage. The configuration accommodates up to 60 passengers in a single class. The landing gear is retractable with the nose and main gear in twin wheel configuration. The power plant is a Composite Cycle Engine (CCE) with an Ultra-High Bypass Ratio (UHBPR) [10]. The flight control system is a 3-axis Fly-by-Light system, electrically actuated and employing full envelope protection. The aircraft is designed to comply with CS-25 and FAR 25 airworthiness regulations and adheres to 90 minutes Extended Twin Operations (ETOPS). Figure 2 presents an artist's illustration of the aircraft concept.

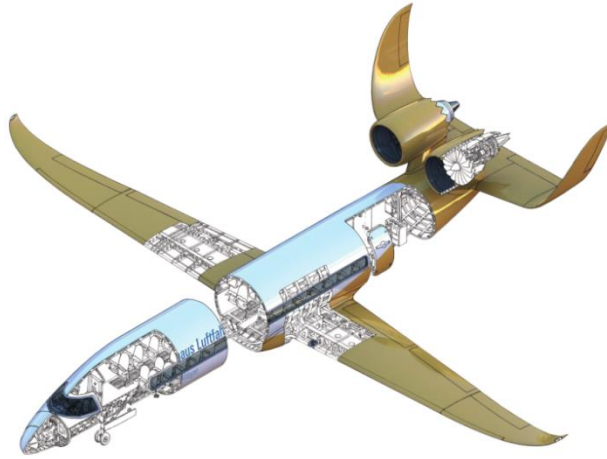


Figure 2: Artist's illustration and overview of technical features

The configuration is driven by the many requirements set for the project. Main drivers were the necessities for Short Takeoff and Landing (STOL) and low noise emission to enable inner-city operation. Furthermore, the compatibility with the inner-city airport, as well as conventional airport and increased fuel efficiency compared to a year 2000 reference has to be ensured. Synergies were created in terms of low speed performance. The low approach speed enables short LFL and also reduces the aircraft source noise, since the major airframe noise sources grow very strong, with powers between 4.5 to 6 [11] to the flight speed. Equation (1) shows that a 20 % reduction in approach speed leads to a reduction of 6 dB overall aircraft noise [12]:

$$\Delta L = 55 \cdot \log_{10} \left( \frac{V_{APP_{new}}}{V_{APP_{ref}}} \right) \quad (1)$$

The STOL requirement stands contrary to cruise efficiency and low noise emissions. A STOL design in general can be enabled through an efficient high lift system, a low wing loading and low sweep. An efficient high lift system that produces a high maximum lift coefficient generally has a high noise signature (e.g. multi-slotted flaps and slats) [12, 13, 14]. Figure 3a (overleaf) shows that a wing loading of 450 kg/m<sup>2</sup> would not only lower the Maximum Takeoff Weight (MTOW) by 2 % compared to a wing loading of 350 kg/m<sup>2</sup>, but also increases the Specific Air Range (SAR) by 6.2 %. The unswept wing was chosen to enable good low speed performance [15] but lowers the cruise speed due to a lower critical Mach number described in the simple wing sweep theory [15].

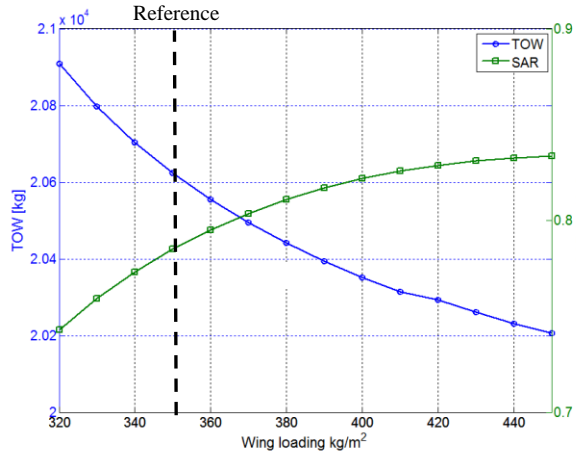


Figure 3a: Change of TOW and SAR with wing loading

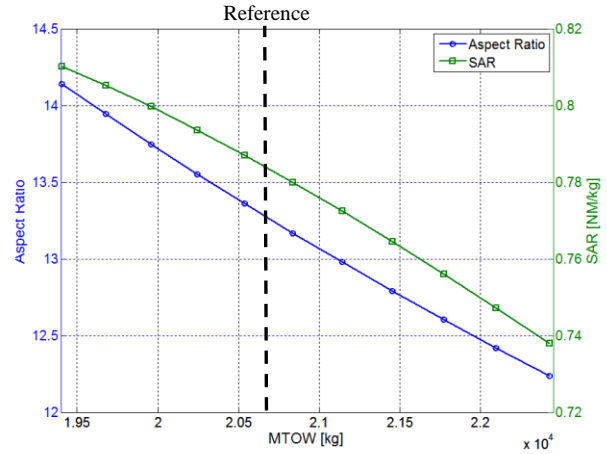


Figure 3b: Impact of a change in MTOW on aspect ratio and SAR

Key driver for the engine positioning has been the benefit through noise shielding, that offers a significant reduction potential [16, 17] on noise intensities, especially below the aircraft. The engine was positioned on the aft upper fuselage outside the fuselage boundary layer. In conjunction with the U-tail configuration, the surfaces provided by the fuselage, the horizontal stabilizer and fin deflect the noise coming from the engines. However, the disadvantage of this configuration is an expected higher interference drag of the overall aft layout consisting of engines, pylons and empennage and the thrust dependent pitching moment. The side-by-side arrangement of the engines as used in many conceptual studies [17, 12] poses the danger of uncontained engine failure that impairs functionality of the other engine. Mitigation of this failure risk is addressed in [17] by use of high-energy absorbing materials. This imposes a weight penalty on the aircraft, but enables the efficient noise shielding of the engines in the first place. A further way to mitigate the problem is by longitudinal staggering, which was not evaluated during the design process.

Furthermore, a strong dependency comes from the constraints on the aircraft dimensions. Considering a constant wing loading and a maximum span width of 28 m, the MTOW has a direct impact on the aspect ratio and the induced drag, which results in a decreased SAR (Figure 3b). Lowering the MTOW by 1 % (206 kg) increases the aspect ratio by 0.44 % and the SAR by 0.28 %.

The low wing layout and the engine position enable a wing integrated landing gear which is of short length, contributing to a low weight and noise emission. It also reduces the cabin floor sill height. As it is well below 1.8 m (6 feet), the aircraft does not need emergency slides [18].

## 2.1 Airframe Technology Assessment and Selection

As seen in the statistical overview (Table 3), the desired performance of the aircraft in terms of STOL and noise emissions are the most challenging. To resolve this matter, technological advancements need to be implemented. Therefore basic studies of changes in zero-lift drag  $CD_0$ , induced drag  $CD_i$ , maximum lift coefficient  $CL_{max}$ , structural weight and thrust specific fuel consumption TSFC were performed to obtain sensitivities on overall aircraft level and see, if the concept differs in some of the characteristics compared to conventional aircraft. This first analysis automatically sizes the overall aircraft according to the changes but does not include detailed effects of how an improvement is achieved (e.g. lower  $CD_i$  through higher aspect ratio) and how it might affect other parameters such as weight or TSFC. The improvements adhere to the formula for the specific air range (SAR).

$$SAR = \frac{v \cdot L/D}{m \cdot g \cdot TSFC} \quad (2)$$

Figure 4 shows the impact of a change in  $CD_0$  and  $CD_i$  on the SAR at begin of cruise. The  $CD_0$  has a stronger impact on cruise performance than the induced drag improvement. The quasi linear character of the plots offers the possibility to calculate a gradient shown in the diagram. It is clearly visible that the impact of a change in  $CD_0$  is about four times as strong as a change in  $CD_i$ . This ratio is higher than usual, due to the low wing loading for the desired cruise Mach number. It is therefore recommended to improve  $CD_0$  rather than  $CD_i$ . The same analysis with the change of trip fuel, including the overall mission shows the same results, with a slightly less pronounced effect for both  $CD_0$  and  $CD_i$  on a 500 NM off-design mission.

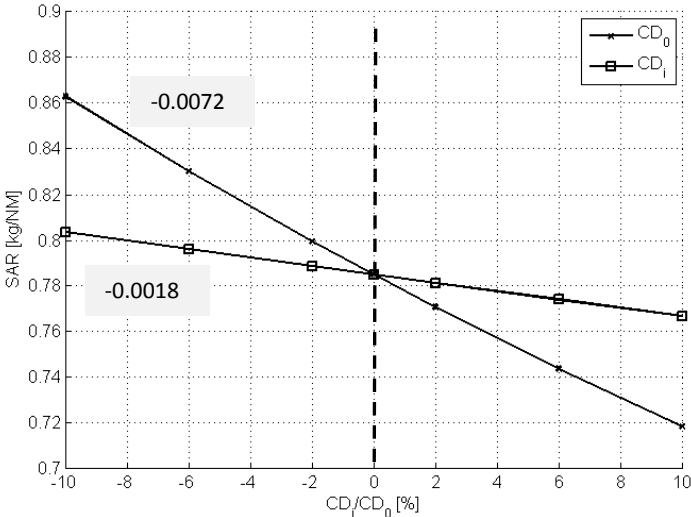


Figure 4: Impact of changes in zero-lift drag  $CD_0$  and induced drag  $CD_i$  on the design mission

Figure 5 shows the effect of an increased maximum lift coefficient on the SAR in cruise. Since wing loading is mainly driven by the runway length constraint, an increase in  $CL_{max}$  could increase wing loading for a constant LFL, thereby increasing cruise performance. The more efficient the high lift system, the higher the SAR value. But as mentioned before, a balanced design is required, since a more efficient high lift system leads most probably to higher noise emissions.

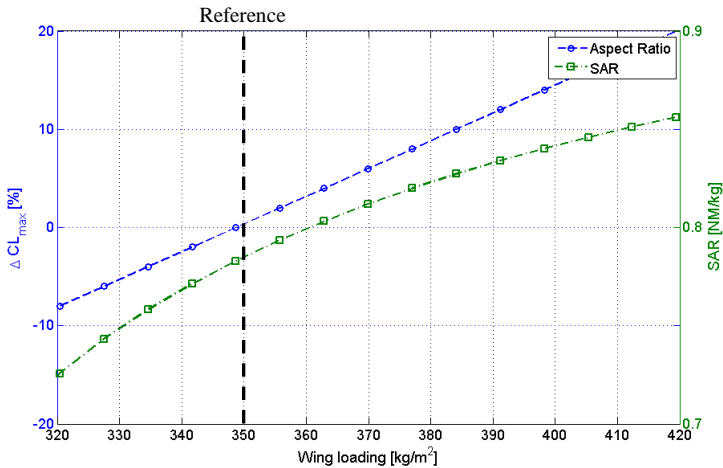


Figure 5: Impact of increased  $CL_{max}$  on SAR with constant LFL

Figure 6 (overleaf) shows the impact of weight and TSFC on the SAR. A significant impact of change in TSFC is shown. A trend that is foreseeable and currently shown in the A320neo attaining most of



its efficiency gain from engine improvements. The impact of structural weight is of low relevance to SAR, even on low range off-design missions.

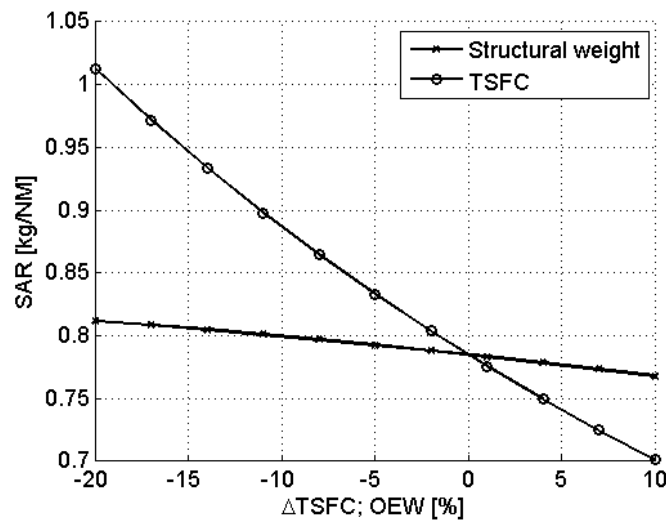


Figure 6: Impact of changes in TSFC and structural weight on SAR

The preliminary analysis serves as a guide on the further implementation of technologies. It indicated strong improvement potential for a higher propulsive efficiency. Furthermore the second strongest effect can be achieved by reducing zero-lift drag. The share of zero-lift drag on the overall drag of this concept is about 50 % higher in cruise flight, than on an A320 for example, causing a bigger impact in the analysis but enabling the required field performance and noise constraints. This is driven by the low wing loading, leading to a higher wing area. Therefore, the share of induced drag is equivalently reduced in cruise flight. This relation offers the possibility that improvements in the maximum attainable lift coefficient will also greatly benefit the overall aircraft performance by simultaneously increasing the wing loading. Therefore, a strong impact between  $CL_{max}$  and  $CD_0$  exists. Since a certain change in  $CL_{max}$  is more easily obtainable than a  $CD_0$  or TSFC reduction in the same magnitude this poses a great potential for improvement. Table 4 shows the summary of the impact through changes analyzed in this preliminary study.

Table 4: Overview of preliminary analysis

| <i>Type</i>              | <i>SAR increase<br/>for ±1%</i> |
|--------------------------|---------------------------------|
| <b>TSFC</b>              | ±0.0092                         |
| <b>CD<sub>0</sub></b>    | ±0.0072                         |
| <b>CL<sub>max</sub></b>  | ±0.0052*                        |
| <b>CD<sub>i</sub></b>    | ±0.0018                         |
| <b>Structural weight</b> | ±0.0015                         |

\*linear approximation at wing loading of 350 kg/m<sup>2</sup>

Based on the analysis a set of technologies was selected to fulfill the requirements. For choosing technologies it was decided to prefer simple and less complex technologies. They are usually lower in weight and maintenance, and provide higher operational reliability. The limited space at the airport and tight ground schedule calls for an aircraft with a high operational reliability.

Due to the high importance of a change in TSFC, a radical engine concept (CCE) was chosen improving this value but also adding weight to the propulsion system. The technology is presented in detail in section 2.3.

The reduction of  $CD_0$  was conducted through two different measures. A natural laminar flow nacelle lowers the zero-lift drag of the nacelle. This technology is already in use today on the Boeing 787 with prospects to further delay the boundary layer transition in future applications [19, 20]. Due to the high bypass ratio of the engine, the wetted area increases, rendering the application of natural laminar flow on the nacelle necessary and reducing trip fuel on the design mission by 2.4 %. The reduction of fuselage drag was a further measure to increase aerodynamic efficiency since it has the biggest share of wetted area on the aircraft. The reduction of the friction coefficient  $C_f$  is possible through different means. An often discussed method is Riblets, which can be almost weight neutral [21] and can be applied on about 70 % of the fuselage. A decrease of 8 % [22] in  $C_f$  can be obtained leading to a reduction of 1.7 % in trip fuel on the design mission. A major disadvantage is the decreasing efficiency over time [23], requiring a high maintenance and cleaning effort. Other drag reduction coatings [24] can be applied alternatively, showing a similar benefit. The application of laminar flow technologies on lifting surfaces would promise further improvements, but was not applied. Natural Laminar Flow implies certain airfoil shapes that most probably contradict with high lift requirements. A hybrid laminar flow control system is a very complex system with operational issues to overcome. Due to the fact, that the required power of the compressor is a function of the ambient air density, the activation of the system will be at or slightly below initial cruise altitude. Therefore no contribution can be expected on climb and descent phases, which makes its utilization on a regional aircraft less efficient than on mid or long range aircraft.

The increase of  $CL_{max}$  is challenging, as it stands contrary to noise reduction demands. This implies that according to [12, 14] multi-slotted fowler flaps, slats or powered lift concepts are not feasible. It was therefore decided to make use of an unswept and, due to aft engine location, uninterrupted wing and install a high lift system that runs along the whole span, excluding the winglet. The leading edge device consists of a sealed Krueger flap with no gap between flap and main wing, and the trailing edge uses a plain flap. To support this, the ailerons can be drooped to act as flaperons like on the Airbus A330/A340 series [25]. To energize the boundary layer for prevention of flow separation, plasma actuators were chosen. Although a technology that is controlled actively, the characteristics promise low demands on the power system design, as well as on maintenance and integration of the technology, therefore providing a comparatively low complexity for an active system. Tests with low Reynolds-numbers have shown an increase of  $CL_{max}$  of up to 20 % [26]. The technology is currently still at a low technology readiness level (TRL) of 4 but offers the advantage that it requires only little power of about 1W/cm along the wingspan [27]. Furthermore, the weight impact appears to be very low as well [28], justifying the use only for operation in the low speed regime and hardly decrease cruise performance. The use of high voltages and frequencies during actuation leads to electromagnetic interference (EMI). The Fly-by-Light technology mitigates this problem only partly, requiring further research on this topic. The maximum lift coefficient of the wing was calculated to be  $CL_{max} = 3$  with the use of plasma actuators. This is a fairly high value for a slotless high lift system. If necessary, the plain flap system can be replaced with a continuous mold-line link flap, increasing lift capabilities compared to a plain flap and still showing a significant noise reduction [29, 30]. In general, the high lift configuration is expected to have very low drag characteristics, improving L/D in takeoff and approach configuration. This enables a better second segment climb performance, thus reducing noise impact on the ground.

Induced drag was reduced using a high aspect ratio wing. Due to the constraint for span width and a required wing loading for field performance, the aspect ratio is 13.31 at a span width of 28 m.

To augment the takeoff process, a catapult system was envisioned assisting the aircraft. This process is outlined in Figure 7. A conventional takeoff would be feasible on the short runway but leads to significantly higher thrust requirement of about 40 %. The engine would be designed for the takeoff case only, adding significant weight to the aircraft, far from the center of gravity (CG). To avoid the additional weight due to higher thrust requirements, an Electromagnetic Aircraft Launch System (EMALS) [31] is used, connected to the aircraft via the forward landing gear. This adds much less structural weight to the aircraft, than sizing the engines for the takeoff case without a ground system.

The system enables a constant acceleration of  $4.8 \text{ m/s}^2$ . The obstacle clearance height at the end of the takeoff was reduced to 3 m (9.8 ft) since the aircraft is already around 40 m (131 ft) above ground level, while on the runway. The rejected takeoff (RTO) case was considered using the EMALS system to assist in braking. An additional rod, connected to the fuselage between the main gears, decelerates the aircraft. Using only the forward rod for braking would destabilize the aircraft during RTO. On normal takeoff, the aft rod has a rotation actuated release mechanism. A deceleration of  $5.5 \text{ m/s}^2$  was found necessary for this case. This deceleration can, for redundancy reasons, also be achieved without the EMALS using the normal braking devices of the aircraft but causing higher wear and heat built up in the brakes.

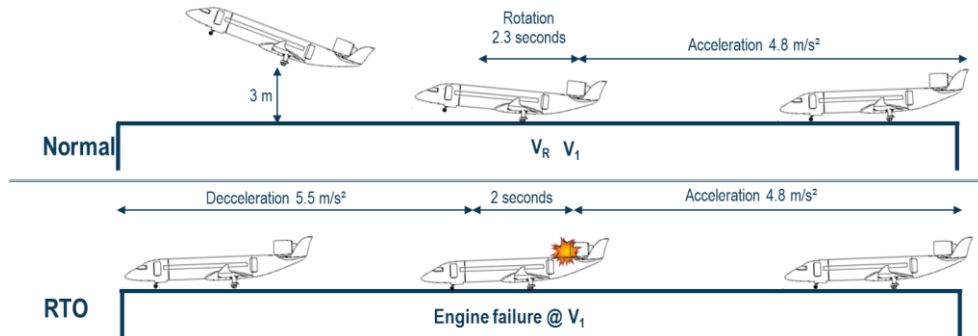


Figure 7: Visualization for normal and rejected takeoff (RTO)

An autoland system with increased navigational capabilities ensures a lower landing field length, due to a lower requirement for touchdown zone length, justifying a lower safety factor than today. A higher approach angle of 5.5 degrees and a slightly increased deceleration of  $4.6 \text{ m/s}^2$  further assist the targeted value of 640 m LFL including safety factors. A ground based emergency braking system proposed by [32] additionally enhances operational safety.

The potential of weight reduction through CFRP has been discussed in many ways as well as the disadvantages [33, 34, 35]. The benefits are manifold and the technology is expected to have matured within the timeframe targeted, so that weight reductions of structures can be as high as 20 % compared to today. The furnishing of the aircraft was also reviewed showing potential for weight saving, for example through materials reducing seat weight [36, 37, 38]. A further weight benefit can be gained by utilizing Fly-by-Light technology, significantly reducing cable weight [39]. It also serves as an enabler for advanced flight control schemes by providing a higher bandwidth. Through the use of CFRP the aircraft is more prone to EMI. The immunity to EMI of the Fly-by-Light system makes it a perfect match for the CFRP structures and has reached the TRL 9 with the Kawasaki P-X aircraft already in service [40].

On subsystem level, an all-electric subsystem architecture is used, eliminating hydraulic and pneumatic systems. This enables a bleedless architecture and a power on demand approach for the engine power offtake, increasing system efficiency and improving maintainability. In contrast, a higher weight has to be accepted. For the aircraft, the following systems are supplied by the electric system:

- Anti-Ice System
- Environmental Control System
- Landing Gear (Steering, extension/retraction, braking)
- Avionics
- Flight controls (primary and secondary)
- Cabin (Galley, Lavatory, Entertainment, Lighting)
- Plasma actuators

For the electric subsystem, a first order estimation based on [41] was conducted to evaluate weight and power requirements of the sub-components. Powers were estimated according to [42, 43] and the mass via specific powers of all sub-components. This concludes to a maximum power offtake of 135 kW per engine and a total mass of the electric system of 1,773 kg.

Table 5 gives an overview of the incorporated technologies and the parameters that the technology is expected to affect in a positive way. It includes the measures taken to reduce the noise emission of the aircraft described hereafter.

Table 5: Overview of technologies

| <i>Type</i>         | <i>Technology</i>      | <i>Primary target value</i> |
|---------------------|------------------------|-----------------------------|
| <b>Aerodynamics</b> | Plasma Actuators       | $CL_{max}$                  |
|                     | NLF nacelle            | $CD_0$                      |
|                     | High AR                | $CD_i$                      |
|                     | Coatings/Riblets       | $CD_0$                      |
| <b>Weight</b>       | CFRP                   | Mass                        |
|                     | Furnishing             | Mass                        |
|                     | Fly-by-light           | Mass                        |
| <b>Subsystems</b>   | All electric subsystem | TSFC                        |
| <b>Propulsion</b>   | Composite Cycle Engine | TSFC                        |
| <b>Noise</b>        | Aircraft configuration | Noise                       |
|                     | Flap edge treatment    | Noise                       |
|                     | Sealed Krueger flap    | Noise                       |
|                     | Acoustic liners        | Noise                       |
|                     | Chevrons               | Noise                       |
|                     | UHBPR                  | Noise                       |

## 2.2 Low Noise Aircraft Technologies

The aircraft's low noise signature is achieved by several measures. The previously mentioned aircraft morphology reduces airframe and engine noise. A general approach was to treat all major noise sources, so that no single component stands out in the overall noise signature during any flight phase. Since it is a conceptual design, detailed noise sources such as cavities were not taken into account. Furthermore, this section explains annexed technologies for noise reduction.

The integration of further technologies to decrease sound generating mechanisms was limited as not to add significant weight or decrease efficiency. Table 5 shows the incorporated technologies. The use of flap edge devices is to reduce the vortex induced noise of the flaps during takeoff and in particular during approach. Different ways to treat the side edges are possible, such as side edge fences [44], porous tips [45], active side edge blowing [46] or continuous mold-line link [29]. A technology that yields almost no impact on weight and aerodynamics with good noise reduction characteristics is the porous side edge. Wind tunnel tests showed a reduction on system level between 0 – 25 dB depending on the Strouhal number and therefore the frequency. The engine was treated with proven technologies. These include Chevrons and acoustic liners. A further benefit comes from the UHBPR engine, reducing noise emissions but also shifting the noise pattern from the aft exhaust to the forward fan noise.

### 2.3 Propulsion System

The propulsion system was designed for the envisaged Entry-Into-Service year 2040. For this time, a fundamental change to the core engine of the propulsion system may be expected in order to meet future emission reduction targets. A promising candidate for future aero engine architectures is the Composite Cycle Engine, synergistically combining turbofan components with a piston engine in the high pressure part of the core engine [10].

To evaluate the applicability and the benefits of such a novel architecture, a reference geared turbofan has been set up first with assumed year 2035 technology level. Detailed modeling of turbofan and CCE are described in [47]. The design point for the engine was set at top of climb (37,000 ft; ISA +10 K; M0.67) with a thrust requirement of 7.61 kN. Cycle studies for the reference engine revealed a well balanced design point for combustion chamber exit temperature  $T_4 = 1700$  K and an overall pressure ratio  $OPR = 49$ . The fuel burn optimum specific bypass thrust  $v_s$  was 80 m/s, implying a fan diameter of 1.36 m (54 in.) and a fan pressure ratio of 1.329. This results in a thrust specific fuel consumption  $TSFC = 12.73$  g/kN/h.

Looking at the CCE, studies covering changes in specific bypass thrust  $v_s$ ,  $OPR$  and  $T_4$  were conducted and are summarized in Table 6. The optimum fuel burn improvement was determined at  $T_4 = 1400$  K and  $OPR = 32$ . The parametric study reveals that specific thrust for optimum fuel burn is between  $v_s = 75$  m/s and 80 m/s. Furthermore, the study shows how fuel burn can be traded against lower noise. The maximum feasible fan diameter is constrained by the installation space, aerodynamic trade-offs and the noise shielding effect from the fuselage that decreases with increasing engine size. The diameter was found to be 1.52 m (60 in.). Therefore, specific thrust can be reduced down to  $v_s = 65$  m/s, reducing source noise by roughly 2.8 EPNdB at the cost of about 0.4 % fuel burn. Therefore, a specific thrust of  $v_s = 65$  m/s was chosen for the final design, providing the best compromise of fuel burn and noise improvement as well as installation space. The resulting fuel burn improvement is 17.4 % with an increase in engine weight of 440 kg compared to the reference turbofan engine, mainly coming from increased fan diameter and from additional piston components in the engine.

Table 6: Parametric studies for specific thrust showing optimum CCE cycles.

| <i>Parameter</i>               | <i>Unit</i> | <i>Value</i> |        |        |        |        |        |
|--------------------------------|-------------|--------------|--------|--------|--------|--------|--------|
| <b>Specific thrust</b>         | m/s         | 85           | 80     | 75     | 70     | 65     | 60     |
| <b>TSFC</b>                    | g/kN/s      | 10.57        | 10.52  | 10.48  | 10.44  | 10.42  | 10.40  |
| <b>Powerplant system mass</b>  | kg          | 1580         | 1613   | 1651   | 1692   | 1739   | 1793   |
| <b>Fan diameter</b>            | m           | 1.33         | 1.37   | 1.42   | 1.47   | 1.52   | 1.59   |
| <b>Fan pressure ratio</b>      | -           | 1.354        | 1.329  | 1.305  | 1.282  | 1.259  | 1.238  |
| <b>ΔFuel burn vs. turbofan</b> | %           | -17.76       | -17.85 | -17.85 | -17.72 | -17.44 | -16.97 |

The engine size has been estimated reviewing existing aircraft engines. The nacelle diameter was estimated by reviewing existing engine nacelles. Former studies revealed that CCE length does not increase compared to turbofan engine length [10]. It was found that nacelle diameter can be expressed as an offset to the fan diameter. The resulting nacelle diameter is 2.01 m (79 in.). For the length of an engine with a geared fan, a linear relation was derived and a resulting engine length of 3.60 m (142 in.) was determined.

## 2.4 Cabin and Fuselage Definition

The aircraft is equipped with four passenger doors (type B) which are larger compared to contemporary regional aircraft. The cabin layout is designed for 60 passengers in a four-abreast arrangement with a 29.5-inch seat pitch (0.75 m). A business configuration with 52 seats and 34 inch (0.87 m) seat pitch would be suited for the maximum design range. Two cabin crew seats are located close to the exits in the forward and aft cabin.

A circular cross-section with an outer diameter of 2.69 m (8.8 ft) and lower floor position improves the passenger flying experience with a cabin height of 1.97 m (77.6 inch). Changes to passenger anthropometrics in 2040, in terms of an increase in average height and waist width, were taken into account during the concept phase. The replacement of overhead-bins with small racks for jackets provides a spacious interior perception comparable with larger narrow-body aircraft. The required storage volume is provided below the cabin floor accessible through a hatch, as illustrated in Figure 8. The underfloor stowage is designed to house IATA standard sized luggage. This volume is not available within the proximity of the center wing box which forces 12 passengers to stow their luggage in the belly hold. The cargo hold, which is mainly used for oversized luggage, is located in the aft fuselage near the bulkhead. The under-seat luggage stowing is realized through a foldable seat concept where the seat pan is pivot-mounted. This allows passenger to stow their luggage while standing in the row which significantly reduces aisle interferences. The seat has a non-recline backrest and a tray table.

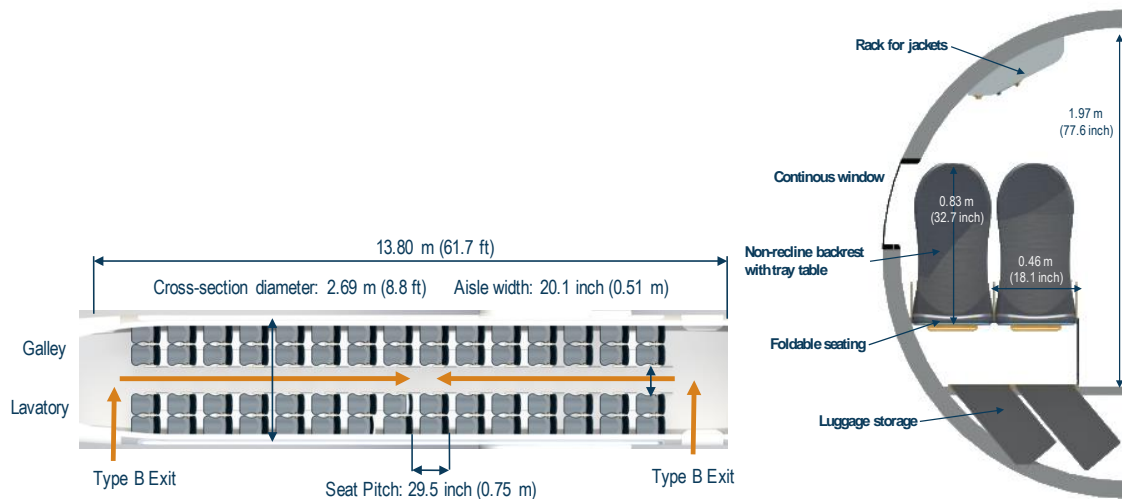


Figure 8: Standard 60 passenger cabin configuration with galley and lavatory in the forward cabin (left) and cross-section with underfloor luggage stowing concept (right)

The galley and lavatory are located in the forward cabin allowing accessibility for flight crew and passengers. The galley is sized for drinks and snacks only. Potable water and waste water is contained in contemporary galley trolleys which enables an easy exchange during catering service. This concept applies also for the lavatory. Hence, a potable water and waste water tank including the piping system becomes redundant allowing an unrestricted positioning of cabin monuments. A variant with galley and lavatory in the back could permit larger monument sizes with a restricted access to the flight crew.

## 3 Performance

The flight performance of the aircraft is divided into several subsections, dedicated to the challenges and constraints of the concept. An acceptable cruise performance has to be realized, while the required field performance and low noise targets have to be achieved. Accelerating the transport time, a faster aircraft turnaround is proposed.

### 3.1 Cruise Performance

General characteristics of the aircraft are presented in Table 7. Basic dimensions and the final layout of the aircraft can be obtained from Figure 9. The aircraft takes full use of the available dimensions defined in the ATLeRs having a span of 28 m and an overall length of 24 m. The metric of Flightpath 2050 using the fuel burn per passenger and distance for evaluation leads to a value of 0.02485 kg/PAX/NM (which translates to 1.68 l/100km).

This amounts to a 29 % reduction compared to an ATR 72-500 and a 53 % reduction compared to an Embraer E170, representing a slower turboprop and a faster jet powered aircraft respectively. Furthermore a year 2000 (Y2000) reference aircraft was set up to evaluate the improvement. Except for the noise constraints, the Y2000 aircraft has to fulfill the same requirements. A reduction of 49 % is reached when comparing with the Y2000 aircraft. Although a significant reduction in fuel and therefore CO<sub>2</sub>, it does not fulfill the requirements defined by the Flightpath 2050 goals interpolated for the 2040 timeframe. A further reduction by 11% or 6 percent points, in relation to the Y2000 platform, has to be achieved to reach the target. The SRIA goals for 2035 regarding the improvements from airframe and propulsion combined (49 %) are just met for the Y2000 reference platform. Increasing this value, a trade-off would be necessary sacrificing other achievements.

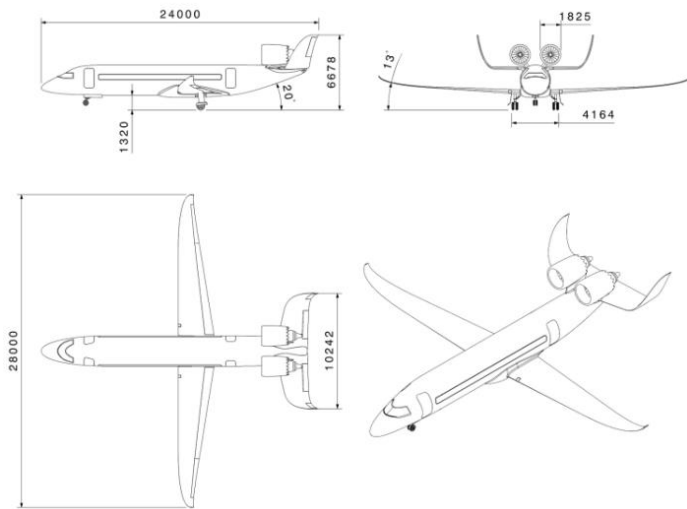


Figure 9: 3-view of the aircraft

Table 7: Parametric review

| <i>Parameter</i>                         | <i>Unit</i>       | <i>Value</i> |
|--|-------------------|--------------|
| <b>Maximum Ramp Weight</b>               | kg                | 20,727       |
| <b>Maximum Takeoff Weight</b>            | kg                | 20,624       |
| <b>Maximum Landing Weight</b>            | kg                | 19,159       |
| <b>Maximum Zero Fuel Weight</b>          | kg                | 18,550       |
| <b>Operational Empty Weight</b>          | kg                | 12,350       |
| <b>Maximum usable Fuel</b>               | kg                | 4,380        |
| <b>Maximum Payload</b>                   | kg                | 6,120        |
| <b>Design Payload</b>                    | kg                | 5,508        |
| <b>Wing Area</b>                         | m <sup>2</sup>    | 58.9         |
| <b>Aspect Ratio</b>                      | -                 | 13.31        |
| <b>Wingspan</b>                          | m                 | 28           |
| <b>Wing loading</b>                      | kg/m <sup>2</sup> | 350          |
| <b>Thrust to Weight</b>                  | -                 | 0.35         |
| <b>Thrust to Weight T/O (with EMALS)</b> | -                 | 0.49         |
| <b>Appr. Speed (MLW)</b>                 | KCAS              | 102          |
| <b>SAR mid cruise</b>                    | NM/kg             | 0.787        |
| <b>Fuelburn per PAX and 100km</b>        | l/100km           | 1.68         |
| <b>Range (LF 90%)</b>                    | NM                | 1,500        |
| <b>Design Range</b>                      | NM                | 1,000        |
| <b>Max. PAX</b>                          | -                 | 60           |
| <b>Ferry Range</b>                       | NM                | 2,200        |
| <b>Cruise Mach number</b>                | -                 | 0.65         |

Figure 10 shows the trade-off that had to be made to meet the field performance and cruise speed requirements resulting from the four hour door to door goal. An efficient long range cruise, defined as 99 % of max. SAR is only at high weights possible and the efficiency reduces during cruise, leading to step climbs. The initial cruise altitude is FL370 and, therefore, higher than usual, especially when considering the regional utilization spectrum of the aircraft. As shown in Figure 3a and Figure 5 the change of wing loading and  $CL_{max}$  can increase cruise efficiency or enable lower initial cruise altitude.

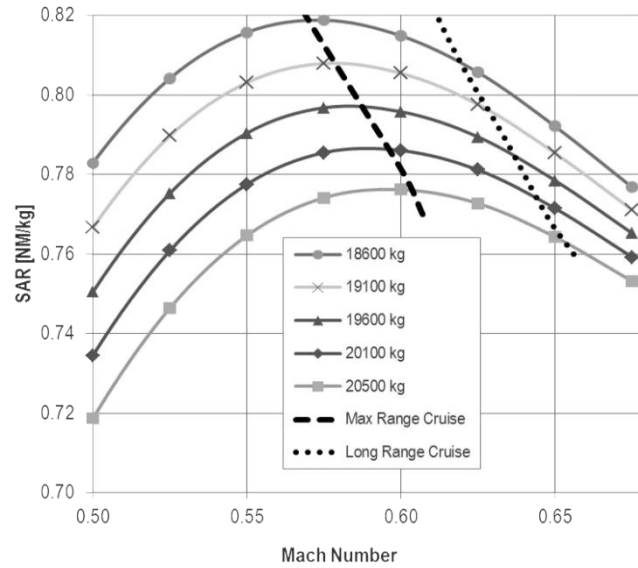


Figure 10: Cruise Speed optimization

### 3.2 Field Performance

The low speed requirements were met achieving a TOFL of 532 m (1,745 ft) using the assisted takeoff system at ISA+10K and a Pressure Altitude (PA) of 2,000 ft, exceeding the required minimum [48]. This provides an additional 20 % safety margin of the runway length.

The landing is not assisted by ground based systems. The reduction of required LFL comes mainly from a steep approach angle, a higher deceleration and the reduction of the safety factor below today's requirement [49], justified by advanced avionics and autoland capability. The value obtained for LFL is larger than for TOFL, leading to a smaller margin of only 16%. For conventional airports, the TOFL and LFL are more than twice as high, even at ISA and mean sea level (MSL). The takeoff without assistance requires 1,080 m (3,543 ft), which fits nicely with the values from comparable aircraft in Table 3. The LFL is 1,182 m (3,878 ft) assuming the normal safety margin, a 3° glide path and a conventional deceleration rate. Table 8 shows an overview of the field performance.

Table 8: Low speed performance summary

| <i>Low speed Scenario</i>                    | <i>Performance Results</i> |          |
|--|----------------------------|----------|
| <b>TOFL augmented @ISA+10, 2000ft PA</b>     | 532 m                      | 1,745 ft |
| <b>Safety factor TOFL augmented</b>          | 1.2                        | 1.2      |
| <b>LFL inner-city ops @ISA+10, 2000ft PA</b> | 553 m                      | 1,814 ft |
| <b>Safety factor LFL inner-city ops</b>      | 1.16                       | 1.16     |
| <b>TOFL conventional @ISA, MSL*</b>          | 1,080 m                    | 3,543 ft |
| <b>LFL conventional @ISA, MSL*</b>           | 1,182 m                    | 3,878 ft |

\*Including safety factors

### 3.3 Low Noise Performance

In order to achieve the required low noise performance a two-fold approach was selected. Firstly, one target is to reduce source noise, thus the noise emission at the aircraft itself, described in section 2.2 and more detailed in [50]. Secondly, another target is to optimize the flight procedures to minimize noise impact on the ground. Both approaches are highly relevant in reducing noise in the vicinity of a city airport and are both pillars of the ICAO's Balanced Approach of Aircraft Noise Management [51].



Generally, aircraft operations show a high potentials to reduce airport noise. This applies both for departures and for approaches. Noise abatement departure procedures, for example, can reduce the noise impact by increased climb rates or by continuous climb procedures. The following will present one promising noise abatement approach procedure that can significantly reduce noise in the vicinity of an airport.

Today, aircraft approaching an airport under instrument flight rules follow the glide slope of the Instrument Landing System (ILS). The current glide slope angle of the ILS is  $3.0^\circ$  at almost all international airports. For the CityBird, a significantly increased glide slope angle of  $5.5^\circ$  is used, as applied at the London City airport. By increasing the distance between emission point and receiver point the sound level on the ground is reduced. Further sound reducing effects may result from a decreased required thrust of the aircraft's engines.

Calculated noise contours of different glide slope angles are presented in Figure 11. The contours show the maximum A-weighted sound level  $L_{Amax}$ . The sound levels are given in respect to a reference sound level  $L_{ref}$ . ( $L_{ref}$  represents a specified noise level as the absolute source noise level of this entirely new aircraft concept is not known. However, the relative differences between the three presented contours due to operational changes are valid.) Different colors represent sound level steps of 5 dB.

Figure 11 shows the corresponding relative sizes of noise contour areas for three different glide slope angles. The results show significant reductions in noise contour areas and thus give evidence of the high noise reduction potential of increased glide slope angles. (Compared to the potential of noise reduction at the source, noise level reduction by increasing the glide slope angle from  $3.0^\circ$  to  $5.5^\circ$  may well be in the same order of magnitude or possibly even higher.)

To conclude, noise reduction by noise abatement approach procedures are a significant and promising means to reduce airport noise. Another obstacle for increased angles of today's aircraft operations lies within the lack of installed navigation systems, e.g. ILS with glide slope angles higher than  $3.0^\circ$ . With an entry into service of 2040, restrictions from navigation systems can be assumed to be overcome as well, e.g. by the introduction of advanced Ground Based Augmentation System (GBAS).

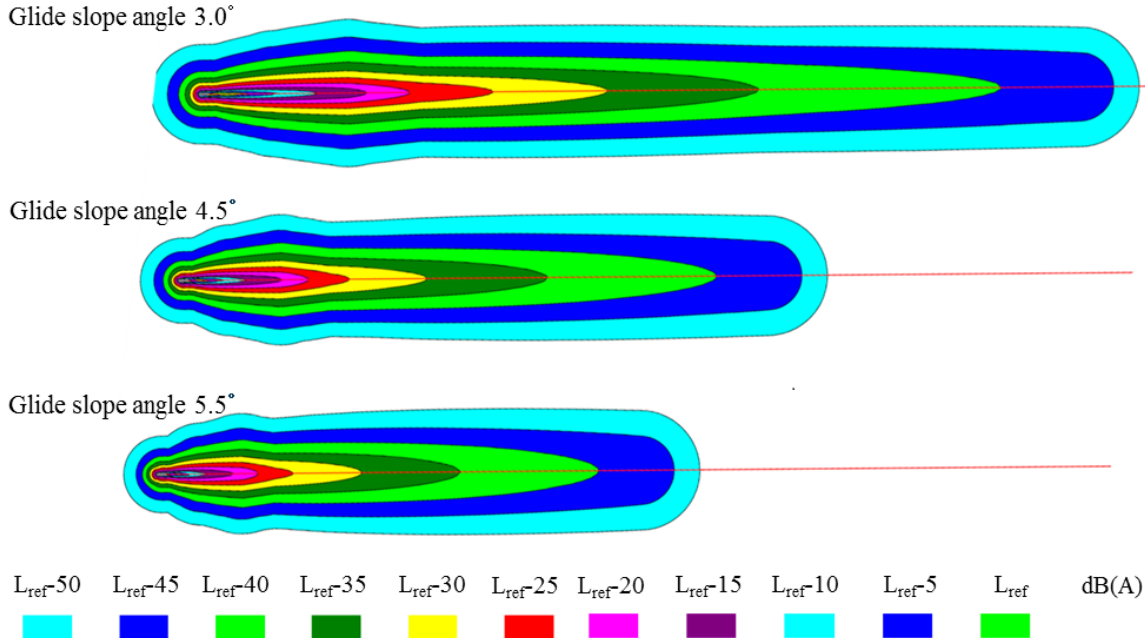


Figure 11: Noise contours ( $L_{Amax}$ ) of different glide slope angles of an approaching aircraft

### 3.4 Aircraft turnaround

The turnaround time is defined as 15 minutes in the ATLeRs which demands a fast passenger boarding and disembarking with simultaneous refueling process. Furthermore, the interface locations are aligned with current best practice [52] and ensure the backwards compatibility with existing airport infrastructure.

Figure 12 illustrates the general ground service arrangement for operations at the inner-city airport. A parallel passenger egress and ingress is allowed using displaceable boarding bridges on the left forward and aft door. The inner-city airport disclaims a baggage sorting system to ensure the challenging ATLeRs in terms of passenger access. Passengers can drop their oversized luggage directly at the aircraft entry in designated zones and ground personnel stows the items in the bulk hold. These procedures are already in place for regional aircraft in service with limited stowage inside the aircraft cabin. Cabin service is provided from the right-hand using stairs. The cleaning is usually performed through the aft door and the catering trolleys are exchanged through the forward door. Waste water and potable water is contained in trolleys and directly connected to lavatory and galley. This enables an unconstrained location selection due to the independency of the piping system and the abolition of extra service equipment. The ground power plug, located at the aircraft nose, and fuel connector at the wing root is automated with a robot-arm attached to a sub-surface supply. The low fuselage height of around 0.5 m enables a fast connection mechanism.

Since the apron layout provides parking positions with boarding bridged on the right-hand and left-hand side, the cross-compatibility is ensured with a redundant ground power connector forward and aft, as well as, fuel connectors for both wings.

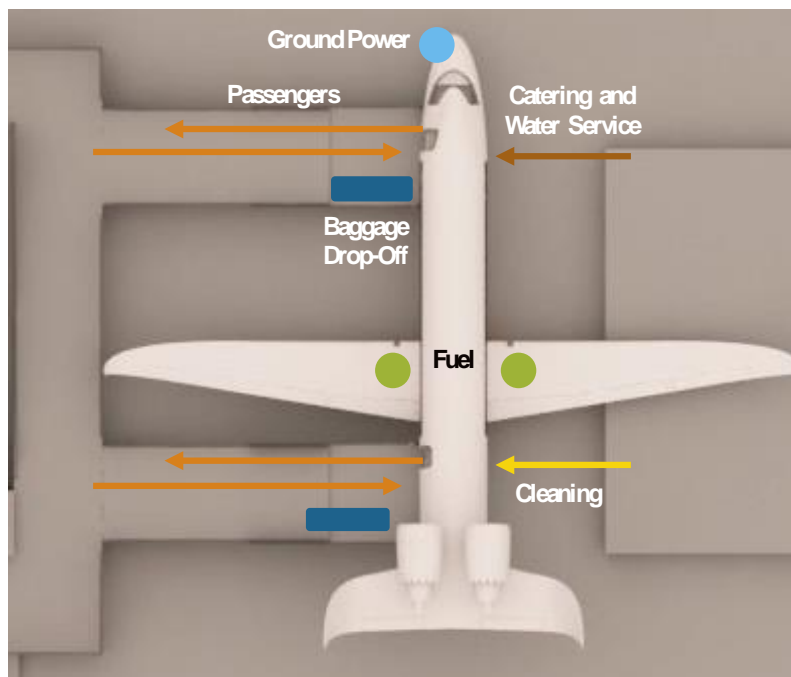


Figure 12: Ground service arrangement at an inner-city airport

The simultaneous passenger boarding and disembarking with the refueling process is enabled through an installed sprinkler system inside the apron level. The Gantt-chart in Figure 13 (overleaf) breaks down the individual process times of the 14 minute turnaround. The automated positioning and removal of the boarding bridges, ground power and fuel connector requires one minute each. The process times are estimated using methods in [53]. The refueling times results in 7 minutes for maximum payload at design range. This takes into account an exponential decrease in fuel flow due to an increasing static pressure in the tank and drag caused by the closing of valves connecting the

installed tanks. The passenger egress and ingress time is based on a passenger flow of 12 PAX/min per door. First studies using an agent-based passenger flow simulation [54, 55] show, that the aforementioned foldable seats could significantly reduce the aisle interferences and required time. For cabin services procedures, the available time without passengers on-board is assumed. Passenger and cabin related processes constitute the critical path.

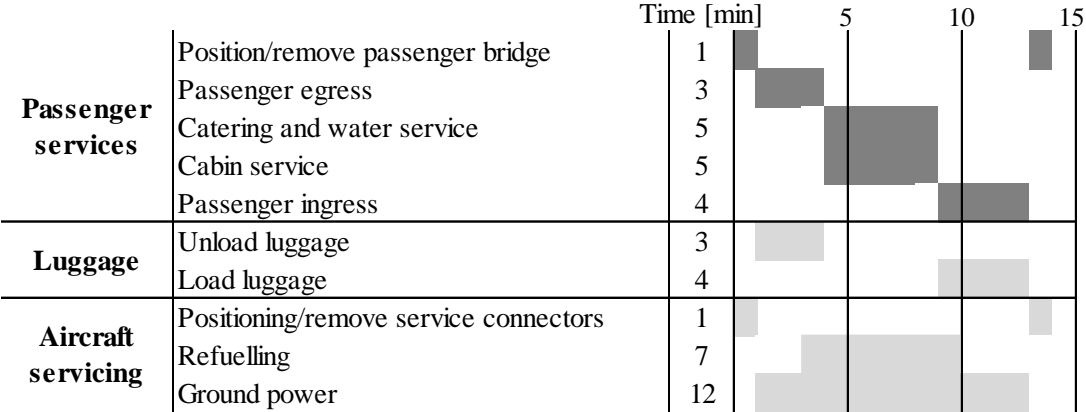


Figure 13: Gantt-chart for a standard 14 minute turnaround. The critical path is highlighted in dark color.

#### 4 Conclusion and future outlook

This paper presented the latest integrated aircraft study from Bauhaus Luftfahrt e.V., dubbed the CityBird. The intent of the design study is to demonstrate a way of achieving the ACARE four hour door-to-door goal and showing the implications on the aircraft. This was accomplished through identification of critical performance values and the application of new technologies. Trade-studies helped defining the final concept.

Future research activities on the platform are manifold. The benefits of an even more efficient high lift system will yield performance improvements. The engines can be optimized to reduce emission, helping to gain acceptance of the proposal, by conducting studies concerning the hybridization of the propulsion system. A family concept with a higher payload and lower range fits very well into the concept increasing passenger flow, still being able to serve most city pairs.

Many measures were taken to achieve a low noise signature. An optimization of dependencies between flight speeds for takeoff and landing, technology impacts and independent behavior of aircraft components probably leads to further improvements [50]. The analysis of even higher approach angles yields a further reduction possibility.

## Acknowledgment

As with all design and integration efforts, this paper is a product of a collective effort. In this instance owing to nature of the problem a good measure of innovative thinking and technical excellence was exhibited by the members of the Bauhaus Luftfahrt Inter-disciplinary Design Team. The following are recognized for their most valued contribution to the CityBird and CentAirStation initial technical assessment exercise:

Valentin Batteiger,  
Julian Bijewitz,  
Ingrid Kirchmann,  
Ulrich Kling,  
Lukas Miltner,

Oluwaferanmi Oguntona,  
Annika Paul,  
Kay Plötner,  
Florian Riegel,  
Arne Roth,

Raoul Rothfeld,  
Christoph Schinwald,  
Michael Shamiyeh,  
Anne Stroh,  
Marcia Urban.

## References

- [1] European Commission, "Flightpath 2050: Europe's Vision for Aviation," Report of the High Level Group on Aviation Research, Publications Office of the European Union, Luxembourg, 2011
- [2] Airbus Global Market Forecast (2012), Boeing Current Market Outlook (2012), ACI Global Traffic Forecast (2012), ICAO: Outlook for Air Transport to the Year 2025 (2005), Rolls-Royce Market Outlook (2009)
- [3] UN World Urbanization Prospects, United Nations, New York, 2010
- [4] Urban M. et al., „CentAirStation - Multi-modal Transport Hub Concept for Inner-city Airport Operation“, Deutscher Luft- und Raumfahrtkongress 2016, 13.-15.9.2016, Braunschweig, Germany
- [5] Schmidt M., Ploetner, K.O. „Forecast Summary,“ internal report from Bauhaus Luftfahrt, IB 2013/ 13008, April 2013
- [6] ACI Global Forecast 2007-2027
- [7] OAG Worldwide Limited, Official Airline Guide Schedules Data, March 2012.
- [8] International Civil Aviation Organization (ICAO), "Annex 16 Environmental Protection", Volume I, Fourth Edition, July 2005
- [9] ACARE, "Strategic Research & Innovation Agenda - Volume 1," 2012
- [10] Kaiser, S., Donnerhack, S., Lundbladh, A., and Seitz, A., 2015, "A Composite Cycle Engine Concept with Hecto-Pressure Ratio," 51st AIAA/SAE/ASEE Joint Propulsion Conference, Orlando, FL, USA
- [11] Dobrzynski W., DLR, "Almost 40 Years of Airframe Noise Research", 14th Aeroacoustics Conference, Vancouver 2008
- [12] Bertsch, E.L.: "Noise Prediction within Conceptual Aircraft Design", PhD thesis, DLR, 2013
- [13] Pollenske M., "Slat noise reduction by means of adaptive leading edge devices," CEAS/XNOISE Workshop, September 2014, Vilnius, Lithuania
- [14] Fischer, M.; Sutcliffe, M.; Friedel, H.; Gölling, B., "Trends for low noisehigh-lift design derived from wind-tunnel tests," ICAS Proceedings 25th congress 2006
- [15] Torenbeek. E. "Synthesis of subsonic airplane design," Delft University Press, 1982
- [16] Dewitte F.H.V., "Aircraft Noise Shielding," Master Thesis, TU Delft, January 2016, Delft
- [17] Frota J. et al, New Aircraft Concepts Research, "NACRE Final Activity Report," 2011
- [18] European Aviation Safety Agency, Certification Specification, CS 25.810 (a)

- [19] Norris G., Boeing plans plain grey natural laminar flow nacelles for 787s in bid to reduce fuel burn” Flight International, November 2006; URL: <https://www.flightglobal.com/news/articles/picture-boeing-plans-plain-grey-natural-laminar-flo-207769/> [cited: 23 May 2016]
- [20] Barry B. et al, “The flight testing of natural and hybrid laminar flow nacelles”, ASME June 1994, The Hague, Netherlands
- [21] Bechert, D. W., Bruse, M., Hage, W., & Meyer, R., “Fluid Mechanics of Biological Surfaces and their Technological Application,” *Naturwissenschaften*, 87(4), 157–171, 2000
- [22] Reneaux, J., “Overview on drag reduction technologies for civil transport aircraft,” ECCOMAS, 2004
- [23] Stenzel V., Wilke Y., Hage W., “Drag-reducing paints for the reduction of fuel consumption in aviation and shipping. *Progress in Organic Coatings*,” 70(4), 224–229. 2011
- [24] Triple O performance solution, Creekmoor, United Kingdom, 18.05.2016 URL: <http://www.tripleops.com/benefits-technical.php>, [cited: 23 May 2016]
- [25] Sforza P. M., “Commercial Airplane Design Principles,” 1st edition, 2014, Elsevier Reference Monographs
- [26] Grundmann S., Frey M., Tropea C., „Unmanned aerial vehicle (UAV) with plasma actuators for separation control,“ in: AIAA-2009-698; 47th AIAA Aerospace Science Meeting (2009) Orlando, Florida
- [27] Kriegseis, J., “Performance Characterization and Quantification of Dielectric Barrier Discharge Plasma Actuators,” PhD Thesis, TU Darmstadt, 2011, p. 26
- [28] Opatis, D.F., “Dielectric Barrier Discharge Plasma Actuator for Flow Control“, NASA, Final Report, NASA/CR-2012-217655, September 2012
- [29] Qing A., University of Bristol, „Airfoil noise reduction using morphing trailing edge,” The 21st International Congress and Sound and Vibration, Beijing, 2014
- [30] Hutcheson F., Brooks T., Humphreys W., "Noise Radiation from a Continuous Mold-Line Link Flap Configuration", 14th AIAA/CEAS Aeroacoustics Conference (29th AIAA Aeroacoustics Conference), Aeroacoustics Conferences, 2008
- [31] Patterson, D., “Design and Simulation of an Electromagnetic Aircraft Launch System”, DOI: 10.1109/PSEC.2002.1022384 Conference: Power Electronics Specialists Conference, 2002. pesc 02. 2002 IEEE 33rd Annual, Volume: 3
- [32] Matthew A. et al., „Developing Improved Civil Aircraft Arresting Systems,” Airport Cooperative Research Program Report 29, 2009, Chapter 14
- [33] Bräutigam K.-R., Achternbosch M., “Analyse der Umweltauswirkungen bei der Herstellung, Nutzung und Entsorgung von CFK-bzw. Aluminiumrumpfkomponten im Flugzeugbau,” *Tech. - Theor. und Prax.*, vol. 12, no. 1, pp. 87–92, 2003.
- [34] Achternbosch M., et al., “Material flow analysis - a comparison of manufacturing of CFRP-fuselage-components versus aluminium-fuselage-components for commercial airliners,“ *Fresenius Environmental Bulletin* 12(2003)6, p. 656-662
- [35] Amendola, A., “Future aerostructure for the next generation green civil aircraft”, Alenia Aeronautica, Aerodays 2011, Madrid
- [36] RECARO Aircraft Seating, “SL3510 - The slim lightweight seat for short-haul flights," URL: <http://www.recaro-as.com/produkte/economy-class/sl3510.html>, 2016. [cited: 23 May 2016]
- [37] Pitch Aircraft Seating, “Introducing the Pitch PF2000," 2016, URL: <http://www.pitchaircraftseating.co.uk/>[cited: 23 May 2016]
- [38] Kuhnla W.-D., “Innovations and Advanced Technologies for the Future Cabin System," Altair Technology Conference, 2011.
- [39] Todd J. R.; “Fly-by-Light Technology Development Plan”, NASA Contractor Report 181954, August 1990

- [40] Kawasaki Heavy Industries website, URL: [http://global.kawasaki.com/en/mobility/air/aircrafts/p\\_1.html](http://global.kawasaki.com/en/mobility/air/aircrafts/p_1.html), 2016, [cited: 31 May 2016]
- [41] Isikveren A.T., "Conceptual Studies of Universally-Electric Systems Architectures Suitable for Transport Aircraft," Deutscher Luft- und Raumfahrtkongress 2012, Berlin, Germany
- [42] Vratny P. C., "A Battery Powered Transport Aircraft," Saarbrücken: AV Akademikerverlag, 2012.
- [43] Xia X., "Dynamic Power Distribution Management for All Electric Aircraft," Cranfield University, 2011.
- [44] Leifsson, L.T., PhD Thesis, Virginia State University; „Multidisciplinary Design Optimization of Low-Noise Transport Aircraft," 2005
- [45] Angland D, University of Southampton, „Measurements of Flow around a Flap Side Edge with Porous Edge Treatment," AIAA Journal, Vol. 47, No. 7 (2009)
- [46] Hutcheson F.V., NASA Langley Research Center. „PIV measurements on a Blowing Flap“, AIAA
- [47] Kaiser S., Seitz A., Vratny P., Hornung M., "Unified Thermodynamic Evaluation of Radical Aero Engine Cycles", ASME Turbo Expo 2016, GT2016-56313, Seoul, South Korea, 2016
- [48] Joint Aviation Authorities, Joint Aviation Requirements, JAR OPS 25.113
- [49] Joint Aviation Authorities, Joint Aviation Requirements, JAR OPS 1.515
- [50] Heinemann P., Shamiyeh M., Plötner K.O., Jeßberger C., Hornung M., (2016): Conceptual studies of a transport aircraft operating out of inner-city airports, abstract for a paper proposal submitted for the DLRK 2016 accepted
- [51] ICAO, Doc 9829, "Guidance on the Balanced Approach o Aircraft Noise Management," First Edition, 2004
- [52] Schmidt M., Nguyen P., and Hornung M.: Novel Aircraft Ground Operation Concepts Based on Clustering of Interfaces, SAE Technical Paper 2015-01-2401, Seattle, Washington State, USA. doi:10.4271/2015-01-2401.
- [53] Schmidt M., Paul A., Cole M., Plöetner, K.O., "Challenges for ground operations arising from aircraft concepts using alternative energy," Journal of Air Transport Management, doi:10.1016/j.jairtraman.2016.04.023.
- [54] Schmidt, M., Engelmann, M., Brügge-Zobel, T., Hornung, M., and Glas, M., "PAXelerate - An Open Source Passenger Flow Simulation Framework for Advanced Aircraft Cabin Layouts," 54th AIAA Aerospace Sciences Meeting, American Institute of Aeronautics and Astronautics, San Diego, California, USA, 2016. doi:10.2514/6.2016-1284
- [55] Schmidt, M., Engelmann, M., Rothfeld, R. and Hornung, M., "Boarding Process Assessment of Novel Aircraft Cabin Concepts", 30th International Congress of the Aeronautical Sciences (ICAS), Daejeon, South Korea: 2016